Article

Precise Estimation of Sugarcane Yield at Field Scale with Allometric Variables Retrieved from UAV Phantom 4 RTK Images

Qiuyan Huang [1,2], Juanjuan Feng [1], Maofang Gao [3,*], Shuangshuang Lai [4], Guangping Han [5], Zhihao Qin [1,3], Jinlong Fan [6] and Yuling Huang [1]

[1] Key Laboratory of Remote Sensing for Subtropical Agriculture, School of Geographical Sciences and Planning, Nanning Normal University, Nanning 530100, China; hqy@nnnu.edu.cn (Q.H.); juanj_feng@email.nnnu.edu.cn (J.F.); qinzhihao@caas.cn (Z.Q.); yuling_h@email.nnnu.edu.cn (Y.H.)

[2] Key Laboratory of Environment Change and Resources Use in Beibu Gulf, Mininstry of Education, Nanning Normal University, Nanning 530100, China

[3] State Key Laboratory of Efficient Utilization of Arid and Semi-Arid Arable Land in Northern China, Institute of Agricultural Resources and Regional Planning, Chinese Academy of Agricultural Sciences, Beijing 100081, China

[4] School of Natural Resources and Surveying, Nanning Normal University, Nanning 530100, China; lsspenny@nnnu.edu.cn

[5] Guangxi Zhuang Autonomous Region Institute of Natural Resources Remote Sensing, Nanning 530023, China; pzhpzh@email.nnnu.edu.cn

[6] National Satellite Meteorological Center, Beijing 100081, China; fanjl@cma.gov.cn

* Correspondence: gaomaofang@caas.cn

Abstract: The precise estimation of sugarcane yield at the field scale is urgently required for harvest planning and policy-oriented management. Sugarcane yield estimation from satellite remote sensing is available, but satellite image acquisition is affected by adverse weather conditions, which limits the applicability at the field scale. Secondly, existing approaches from remote sensing data using vegetation parameters such as NDVI (Normalized Difference Vegetation Index) and LAI (Leaf Area Index) have several limitations. In the case of sugarcane, crop yield is actually the weight of crop stalks in a unit of acreage. However, NDVI's over-saturation during the vigorous growth period of crops results in significant limitations for sugarcane yield estimation using NDVI. A new sugarcane yield estimation is explored in this paper, which employs allometric variables indicating stalk magnitude (especially stalk height and density) rather than vegetation parameters indicating the leaf quantity of the crop. In this paper, UAV images with RGB bands were processed to create mosaic images of sugarcane fields and estimate allometric variables. Allometric equations were established using field sampling data to estimate sugarcane stalk height, diameter, and weight. Additionally, a stalk density estimation model at the pixel scale of the plot was created using visible light vegetation indices from the UAV images and ground survey data. The optimal stalk density estimation model was applied to estimate the number of plants at the pixel scale of the plot in this study. Then, the retrieved height, diameter, and density of sugarcane in the fields were combined with stalk weight data to create a model for estimating the sugarcane yield per plot. A separate dataset was used to validate the accuracy of the yield estimation. It was found that the approach presented in this study provided very accurate estimates of sugarcane yield. The average yield in the field was 93.83 Mg ha^{-1}, slightly higher than the sampling yield. The root mean square error of the estimation was 6.63 Mg ha^{-1}, which was 5.18% higher than the actual sampling yield. This study offers an alternative approach for precise sugarcane yield estimation at the field scale.

Keywords: crop yield estimation; UAV remote sensing; sugarcane farming; allometric variables; crop canopy surface model

1. Introduction

The precise estimation of sugarcane crop yield on a field scale was urgently required by both sugar processing factories and sugarcane farmers [1–6]. The sugar factory required the information to plan its processing schedule according to raw materials from its hinterland. On the other hand, sugarcane farmers are also required to estimate their farming income. The final product of sugarcane farming is the crop's stalk as raw material for sugar factory processing to produce the main product sugar and other by-products such as papers and alcohol. China is recognized as the third-largest sugarcane producer on a global scale. South China is a concentrated sugarcane cultivation area, but the land of each farmer is relatively small (most of them less than a half hectare). In order to have a good schedule of processing, sugar factories usually had to make a rigid schedule for its processing during the sugarcane harvest season, which was usually from December of the year to early March of the following year. This arrangement usually included how many tons of sugarcane were required for timely transport to the factory for processing and which fields of sugarcane cropping regions in the hinterland were felled in time series. Moreover, the local government departments in charge of sugarcane farming and sugar processing and the business persons/organizations might also be interested in the precise estimation of sugarcane production on a regional scale, because they might use this information to formulate suitable policies impacting the farming or to make their decision on sugar business and other relevant business, such as the special fertilizers for sugarcane farming.

Conventionally, sugarcane yield and production were carried out by the cropping technicians of sugar mills through the approach of so-called ground scouting to sample and roughly estimate the yield in the fields [2,3]. This estimation usually unavoidably involved significant errors due to its limitation in taking the samples and visiting the fields. Moreover, the sampling was also high-cost and time-consuming because it needed to have the statistical significance of sampling for regional estimation. Another factor leading to the significant error in the conventional approach was the spatial heterogeneity of sugarcane growing in the regions even in the fields. With the development of remote sensing technology, accurate estimates of sugarcane yield and production became possible at both regional and field scales. In recent years, remote sensing has been the mainstream tool for sugarcane yield and production estimation [3].

Previous studies have utilized satellite remote sensing data [1] and airborne remote sensing data [2–5,7] to estimate sugarcane yield. Though satellite remote sensing has advantages for crop estimation, there are still some challenges in estimating sugarcane yield at plot scale. The first challenge was the inability to obtain high-quality remote sensing images of sugarcane farming due to the influence of unfavorable weather conditions because the farming was mainly distributed in the south subtropical regions of China, where cloud cover was a common sky phenomenon, leading to the difficulty of having satellite images with clear sky condition. Moreover, existing approaches from remote sensing data using vegetation parameters like NDVI and LAI also have several limitations. In the case of sugarcane, crop yield is actually the weight of crop stalks in a unit of acreage. The NDVI's over-saturation during the vigorous growth period of crops results in significant limitations for sugarcane yield estimation using NDVI.

Unmanned aerial vehicles (UAV) have developed very rapidly in recent years due to their conveniences and the low cost for many applications [8,9]. It had been commonly understood that UAV remote sensing had been steadily rising into a new area of remote sensing studies in recent years. The UAV remote sensing platform can provide an alternative approach for estimating sugarcane yield and production at a field scale. It offers a range of distinct advantages, including easy mobility, simple operation, the ability to collect data on demand even in challenging weather conditions, and a high level of spatial resolution. Some studies have explored the applicability of UAV platforms in acquiring very-high-spatial-resolution images for various applications [3–5]. Specifically, Som-ard et al. [3] used a single-phase UAV RGB image to combine with ground sampling data for sugarcane yield estimation. Sanches et al. [4] reported that the green-red vegetation index (GRVI) computed

from their UAV RGB image had a close correlation with sugarcane yield ($R^2 = 0.83$). Sumesh et al. [5] applied the extracted vegetation indices from their UAV-acquired RGB images to integrate with crop surface modeling and object-oriented image analysis for sugarcane yield estimation, demonstrating the potential of UAV RGB imagery in field-scale sugarcane yield estimation. It has been reported that high accuracy of sugarcane yield estimation could be achieved by fusing the sugarcane plant height information obtained from UAV images with the SWAP model [6]. Several studies have shown that sugarcane yield parameters such as tiller number, plant height, and stalks could be efficiently estimated using UAV LIDAR and UAV multispectral image data for accurate plot scale sugarcane yield estimation [7–9]. Akbarian et al. [10] and Barbosa-Júnior et al. [11] examined the combination of multispectral UAV imagery with several machine learning methods for plot-scale sugarcane yields estimation and showed that the random forest algorithm had the best accuracy for the estimation. Though these studies demonstrated the possibility of accurate plot-scale estimation of sugarcane yield and production, problems such as workload reduction, lossless sampling, and fast and accurate estimation are still remained as challenges which required effective solutions [6,10].

It has been commonly understood that various parts of crop plants had their inherent relationship during the growing period, though the relationship might not be identical in different growing stages [12]. This relationship between various parts of crop plants could be expressed as allometric growth equations, which could be used as a non-destructive approach for crop yield estimation [13]. It has been demonstrated that integration of high-resolution satellite images and UAV images with allometric growth equations for different crop types could quickly realize an accurate estimation of crop aboveground biomass and yield, such as in coffee yield estimation [14] and forest biomass estimation [15]. However, the application of this approach to sugarcane farming for yield estimation has not been wisely examined [16]. Recently, Hiernaux et al. [12] used high-resolution satellite images to extract African tree crowns and tree height so that allometric growth equations for leaf and wood and root dry matter could be established for the estimation of the dry mass of woody plants in the Sahel region of Africa. Tucker et al. [17] combined remote sensing images with an allometric growth equation to estimate the forest carbon stock of African drylands [17]. De Carvalho et al. [13] examined the allometric relationships of sugarcane stalk fresh weight (SFB, kg) and total aboveground dry biomass of sugarcane with the plant height and diameter for different sugarcane varieties in Brazil and concluded that allometric growth equations could be used as an alternative approach for precise sugarcane yield estimation.

Guangxi Zhuang Autonomous Region is the biggest sugarcane farming province, and hence, the biggest sugar producer in China. Sugarcane farming in Guangxi had a scale of 857.8 thousand hectares of cropping acreage, 7365.1 thousand tons of sugarcane production, and 6119 thousand tons of sugar production in 2021, accounting for 65.18%, 69.5%, and 77.6% of China's total, respectively [18]. There are more than 70 sugar factories in Guangxi, which usually require precise estimation of sugarcane production in their hinterland for planning the harvest, transportation, and processing schedules.

The objective of this study is to explore the applicability of UAV remote sensing for precise estimation of sugarcane yield and production with the allometric approach at field scale in Guangxi. The major scientific contribution of this study in comparison with current UAV remote sensing applications is that we intend to demonstrate a novel approach for sugarcane yield estimation through the allometric equations and the crop variables, such as stalk density and stalk heights estimated from the UAV images, while the current approaches were mainly conducted through the application of the relationship between the sampling yield and the vegetation indices extracted from the remote sensing imagery. To demonstrate this allometric approach for sugarcane field estimation at a field scale, an experiment was conducted on Dongfeng Sugarcane Farming Base in Wuming District of Nanning Municipality, Guangxi. The DJI UAV with a high-quality camera onboard was used for the imaging campaigns before and after harvest. The acquired UAV photos were

then used to generate high-resolution images of the study region. The UAV images of the crop canopy surface model (CSM) and ground surface model (GSM) were obtained from the above UAV images. Using the CSM and GSM, we calculated the height of sugarcane stalks in the experimental fields for yield estimation. The presentation of the study was organized as follows: The study region and the methodology were outlined in Section 2. Results and analysis were presented in Section 3, which was followed by discussion and conclusions in Sections 4 and 5, respectively.

2. Materials and Methods

2.1. The Study Region

The study was conducted at Dongfeng Sugarcane Farming Base located in Wuming District of Nanning Municipality, Guangxi Zhuang Autonomous Region in southern China (Figure 1). Geomorphologically, the Farming Base resides on low hills stretching from the west to the east in the region, which is weathered from the Karst stratum. The soil in the sugarcane farming fields is typical krasnozem, the red soil formed from the weathered Karst rock layers. The climate of the region is a typical subtropical monsoon pattern, with lots of rains in the hot summer that is very suitable for growing crops such as rice, sugarcane, and citrus. Annual precipitation of the region is about 1400 mm, with over 60% falling during the summer months from June to August, leading to the frequent happening of seasonal drought in spring and autumn [19]. The annual mean air temperature is 22.19 °C, with the high air temperature to be above 35 °C usually in hot summer months, especially July and August, and the low air temperature in January to be about 15 °C. Therefore, the natural conditions of the region are very suitable for sugarcane cropping. Actually, Nanning Municipality, including Wuming District, is the top three sugarcane farming concentration regions in Guangxi Zhuang Autonomous Region. The Farming Base as a business entity is affiliated with the Dongfeng Sugar Company with its sugar processing factory located in Dongfeng town, which is ~10 km from the Farming Base. The fields of the Base were rented from the local village farmers. Previously, the field plots in this region were rather small due to household responsibility policy. After a signed contract with the village farmers to rent the field for sugarcane farming, the small field plots were merged into large ones so that large agro-machinery could conveniently operate. The total sugarcane farming acreage of the Base is about 167 ha, divided into 21 plots. Figure 1b shows the UAV image of the selected experimental fields on the Base.
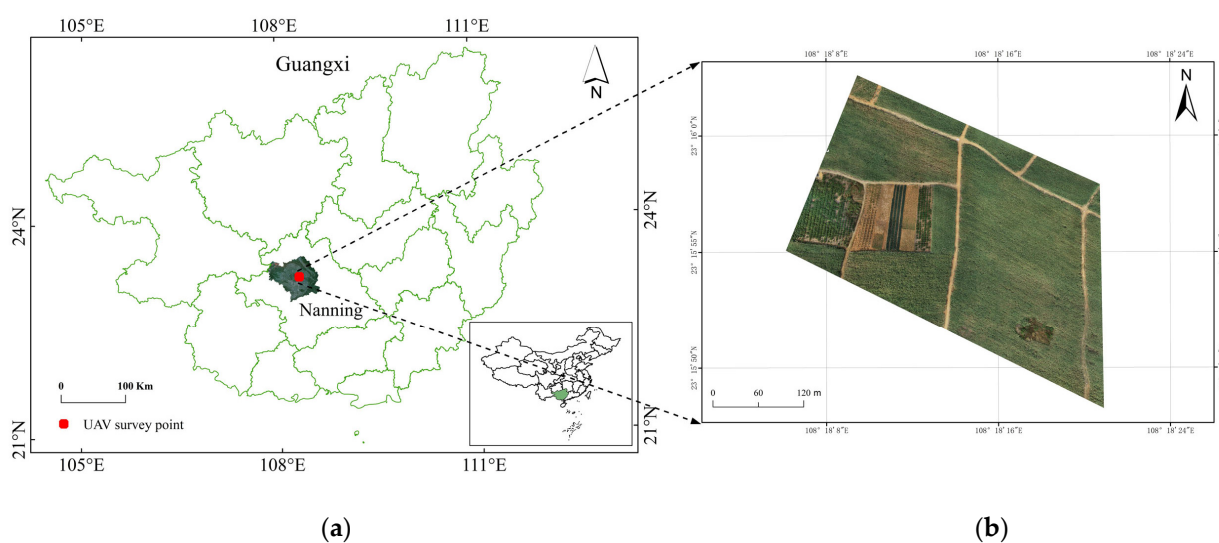

(**a**) (**b**)

Figure 1. (**a**) Geographical location of the study region. (**b**) The unmanned aerial vehicle (UAV) image of the study region in Guangxi, South China.

2.2. Hypothesis and Technical Flowchart of the Study

Crop yield estimation with remote sensing was generally carried out through the approach of establishing the models between the sampling yield and the value of vegetation index especially NDVI or LAI. This is attributed to the fact that crop yield can be viewed as the production of the crop's seed in a unit of cropping acreage, which is actually the direct output of crop growing conditions in the field, while the remotely sensed vegetation index can reflect the general status of crop growing. In our case of sugarcane cropping, the final production is its stalk. This provides an alternative approach to estimating the crop yield of sugarcane farming: to relate the allometric variables such as stalk height or the density of stalk in the field with the final production.

Thus, our hypotheses are that sugarcane yield can be estimated through the physical approach to computing the total weights of sugarcane stalks in the field, provided that the required allometric variables such as stalk height can be estimated from remote sensing with high accuracy (Figure 2).
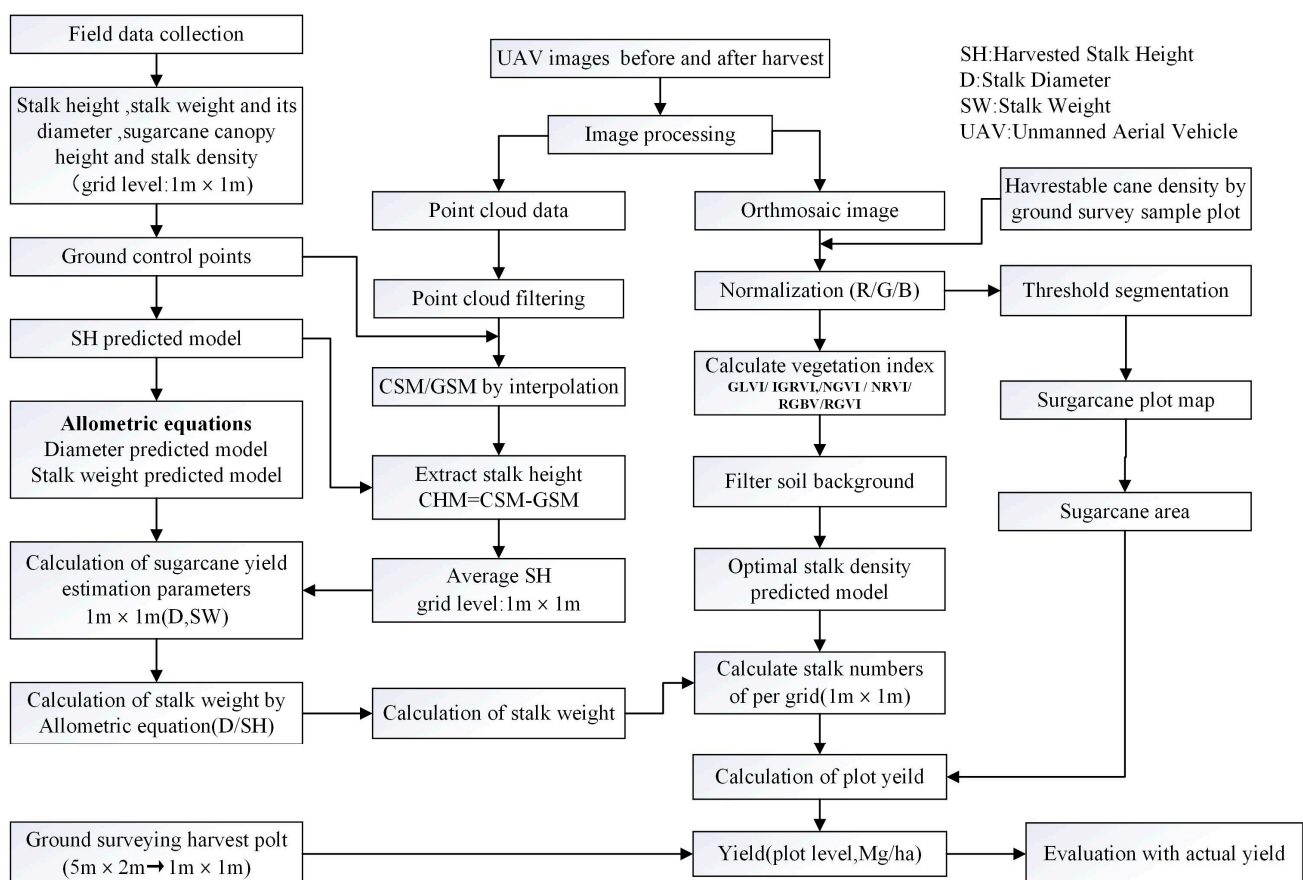

Figure 2. Technical flowchart of the study.

The following procedures were performed in this study.

(1) We performed UAV fight tasks to obtain the UAV photos and to have control points before and after the harvest in the fields; we generated the RGB image from the obtained UAV photos and conducted orthorectification correction of the images for the study region. Details are presented in Section 2.3.

(2) We conducted field sampling campaigns in the fields before harvest to measure required crop variables such as stalk heights, diameter, and so on, for this study. Details are presented in Section 2.4.

(3) We generated the CSM and GSM from the obtained UAV photos for the study region. Details are presented in Section 2.5.

(4) We estimated the stalk height of the fields from CSM and GSM and the harvested stalk height from the stalk height with the allometric equation. Details are presented in Section 2.6.

(5) We calculated the required vegetation indices from the RGB image; we extracted the image value of the vegetation indices for the corresponding sampling points in the fields. Details are presented in Section 2.7.

(6) We established the allometric equation for the variables required for the yield estimation. Details are presented in Section 2.8.

(7) We estimated the stalk density, stalk diameter, and stalk weight with the allometric equations; we estimated the sugarcane yield with the known allometric variables for the entire field. Details are given in Section 2.9.

(8) We validated the yield estimation accuracy. Details are given in Section 2.10.

2.3. UAV Image Acquisition

In this study, we used DJI Phantom 4 RTK (DJI Innovations Co., Ltd., Shenzhen, China) to take photos of the selected sugarcane farming field plots on the Sugarcane Farming Base. A high-quality camera in the visible spectrum range was mounted on the UAV platform to take photos of the ground surface. Two flight campaigns were carried out for the study: one before harvest and the other after harvest. The campaign before harvest was carried out on 15 November 2022 during 12:00–15:30 when the sky was clear without strong wind hence suitable for UAV flight. The other fight campaign was conducted on 12 December 2022 during 11:30–15:00 when it was clear sky. The technical specifications of the UAV camera and the details of the UAV flight campaigns are presented in Table 1.

Table 1. Technical specification of UAV flight campaigns.

Item	Technical Specification
UAV type	DJI Phantom 4 RTK
Viewing angle	90° to the ground
Image sensor	1 inch CMOS, pixels 20 million
Camera lens	FOV 84°; 8.8 mm/24 mm: Aperture f/2.8–f/11
ISO scope	100
Camera focal length	8.8 mm
Photo resolution	W/H 4:3, 4864 × 3648
Positioning accuracy	Vertical 1.5 cm + 1 ppm (RMS), Horizontal 1 cm + 1 ppm (RMS); Note: 1 ppm means that error increases 1 mm for 1 km movement of the vehicle
Duration of flight	30 min
Date of the UAV flight campaigns	15 November 2022 before harvest, and 12 December 2022 after harvest
UAV flight height	45 m relative to the ground surface
Overlapping of imaging	80% along flight direction and 75% between flight directions
Imaging number	1468 photos for 1st campaign on 15 November 2022 and 1520 photos for the 2nd campaign on 12 December 2022
Spatial resolution	0.008 m at the central pixel of the photos

In order to have an efficient mosaic image from the UAV photos, the flight direction of the UAV was set to have 80% overlapping of the photos taken by the UAV camera along the flight direction, while overlapping of the taken photos between two neighboring flights was set to be 75%. The viewing angle for imaging was set to be 90°, i.e., perpendicular to the flight direction. The coordinate system was set as CGCS2000 with a central longitude of 108° E. Camera imaging was set as shutter speed 1/1000 s and sensitivity ISO 100. The flight was carried on in a U-form trajectory for continuous imaging. The flight height of the UAV was set to be 45 m relative to the ground. Therefore, the spatial resolution of the photos was 0.008 m on the central pixel. According to the UAV battery capacity, we conducted several flights with 30 min for each. When taking the photos, the UAV

also simultaneously recorded the position information of the UAV flight, including the coordinates, altitude, and viewing angle of the UAV platform, which was required for laboratory processing of the photos through mosaicing into a continuous UAV image of the fields. In total, 1468 UAV photos were obtained for the 1st flight campaign on 15 November 2022 and 1520 photos for the 2nd campaign on 12 December 2022. During the 1st flight campaign, 19 ground control points along the farmland roads surrounding the fields were measured for calibration of the UAV image (Figure 3). The coordinates and altitudes of the control points were measured with the GNSS RTK surveying device.
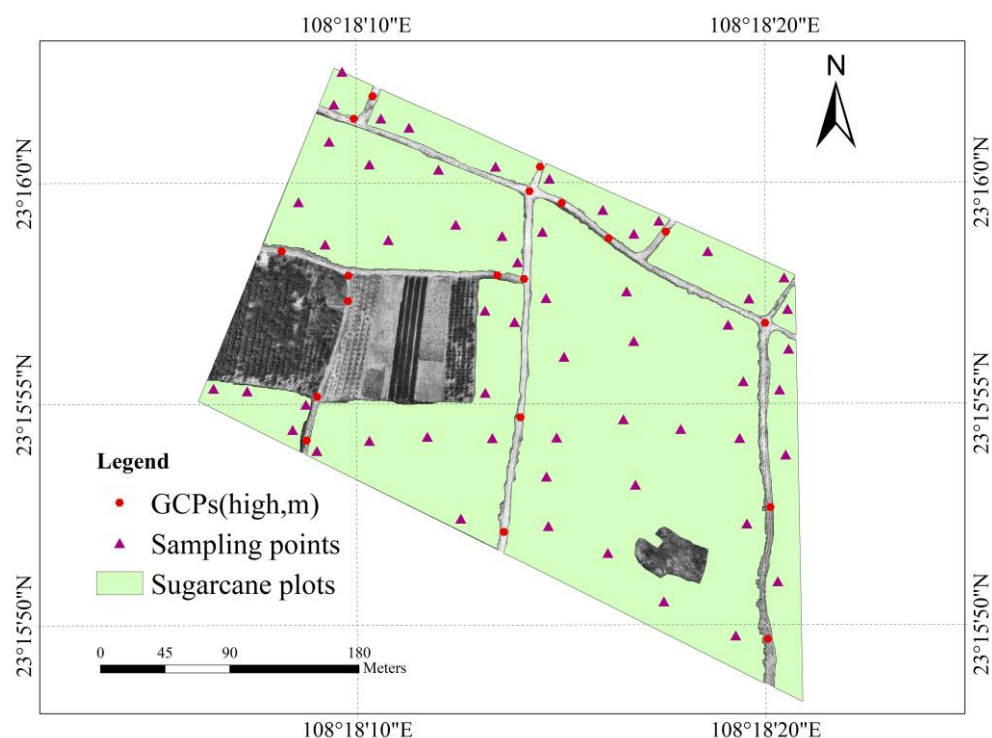

Figure 3. Distribution of the ground control points and the sampling points in the sugarcane fields.

The obtained UAV photos were downloaded to the computer from the camera memory card and then processed in the laboratory by imputing them into the software Lidar360 V6.0.5.0 (Beijing Digital Green Soil Technology Co., Ltd., Beijing, China) to generate the UAV image of the fields, which was completed through mosaicing the obtained UAV photos with the recorded POS data on the imaging position information for each photo. The POS data generally included the camera specification, flight position on a 3-dimensional coordinate, and imaging information. The coordinate system for the mosaicing was set to be CGCS2000 with a central longitude of $108°$ E to match the coordinate system of the UAV photos taken. The UAV image obtained on 15 November 2022 before harvest was used to generate the crop canopy surface model (CSM), while those on 12 December 2022 after harvest were used for the ground surface model (GSM), which was used with the dense point cloud segmentation technique and point filtering method.

2.4. Field Sampling Campaigns

It is necessary to conduct a field sampling campaign to measure plant parameters in the field for yield estimation. Five plant parameters of field sampling measurements were conducted in the study region. Sugarcane stalk density was first measured, and then other parameters including sugarcane canopy height, harvested stalk height, stalk diameter, and stalk weight were measured. For study region, we launched the sampling campaign on the day after the first UAV flight. The sampling scheme was designed in the two cross-section lines of the field that could be the best representative of the sugarcane growing

conditions in the field. In total, we conducted the field measurements of the parameters at 57 sampling sites (Figure 3). For each sampling site, we recorded the coordinates of the site using handheld GPS and measured the sugarcane stalk density, the height of the sugarcane canopy, stalk height, and the diameter of the selected plants that could be harvested.

Sugarcane stalk density cannot be directly measured in the field. Instead, we took the required measurements to calculate the parameter of density, which could be expressed as the number of plants in a unit of cropping acreage. As we all know, sugarcane was normally planted in the type of ridge-liked rows in the fields. Thus, the density could be measured as follows: (1) select two neighboring rows at each sampling site; (2) measure the gap between the rows, i.e., the distance between the two neighboring rows, which in our case was 1.0 m due to the fact that the sugarcane was planted with a planting machine; (3) count the number of sugarcane stalk in the length of 5 m along the two rows; and (4) calculate the density in the laboratory after the sampling campaigns. A total of 57 sampling points were observed for stalk density.

Other parameters were measured by extension tall ruler, caliper, electronic scales, and other tools. An extension tall ruler was used to measure the canopy height and the stalk height of 4–5 sugarcane plants at the sampling site. Usually, sugarcane stalks are not the same size in volume from the bottom to the top. To obtain the average diameter of each stalk under measurement, we used the caliper to measure the diameter at three heights: lower part (usually at ~0.5 m height from the ground), middle part (at ~1.2 m height), and upper part (at ~1.8 m height). Specifically, the stalk diameter was measured in the middle between two knobs at around the measuring height. Since the knob is usually smaller in size than the between-knob part as the major component of the sugarcane plant, this measuring strategy would give us minimal error in using the diameter to compute the volume of the stalk. We chopped down 4~5 sugarcane stalks to measure their canopy height, harvested stalk height and diameter, and stalk weight. A total of 246 sugarcane stalks were chopped for the measurement. Mensurational characteristics of all selected sugarcane stalks for field measurements are presented in Figure 4.
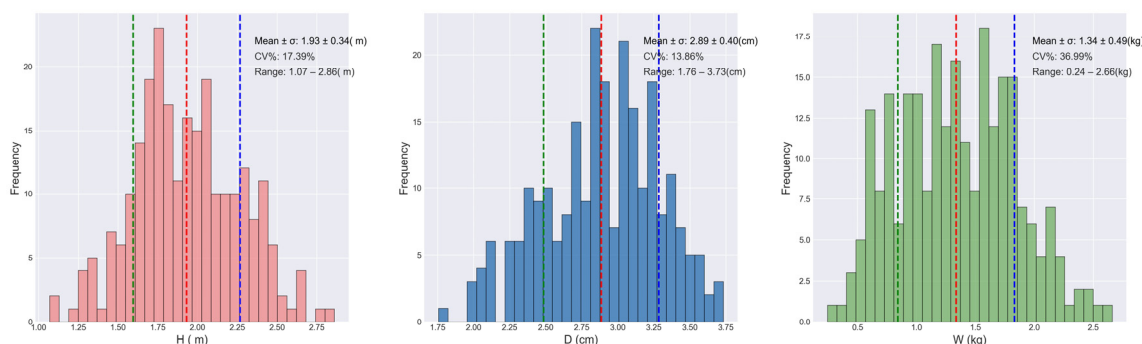

Figure 4. Mensurational characteristics of all selected sugarcane stalks for field measurements. CV in the figure is coefficient of variance, CV = σ/μ, where σ is standard deviation and μ is mean.

2.5. Generation of CSM and GSM from UAV Images

The generation of CSM and GSM from the obtained UAV images was very crucial in the study. CSM and GSM represented the crop canopy surface model and the ground surface model generated with the approach of aerial photogrammetry. The techniques of CSM and GSM generation were quite mature in photogrammetry, and there were several programs for this automatic processing of all the ground points in the photos. In this study, we used the software Lidar360 V6.0.5.0 (Beijing Digital Green Soil Technology Co., Ltd., Beijing, China) with the UAV POS data and the ground control points for the generation of CSM and GSM required for sugarcane stalk height estimation. In order to produce a high-quality CSM and GSM from the acquired UAV photos (Figure 5), point cloud segmentation and point filtering techniques were used in the program to minimize the computation

burden through the generation of point cloud using segmentation to classify the points into groups and to filter the noise information in the generation.
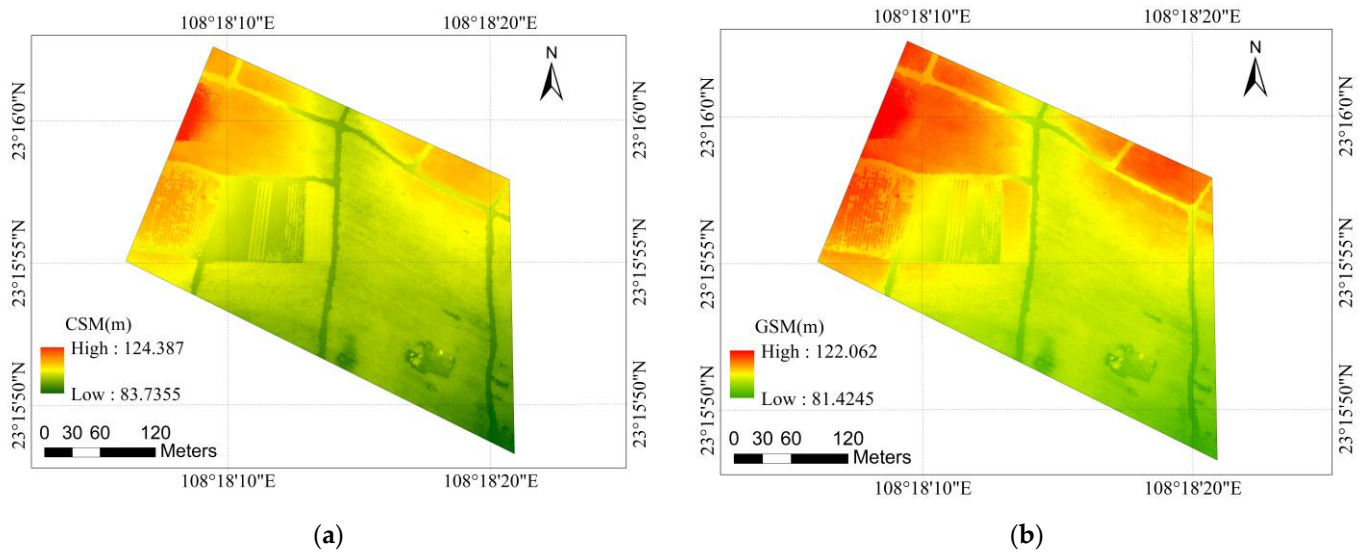

Figure 5. (**a**) CSM (the crop canopy surface model); (**b**) GSM (the ground surface model).

2.6. Estimation of Sugarcane Stalk Height

The height of the sugarcane stalk is a crucial factor for the production estimation of sugarcane farming. Several studies have been published to estimate the crop height from UAV images [20–26]. Generally, this was carried out through the difference between CSM and the GSM of the crop fields generated from UAV images. Guo et al. [20] indicated that the estimated wheat heights from the UAV images had a very high correlation with the actual measured ones through sampling in their experiment. The study of Zhang et al. [24] also proved that the maize height could be precisely estimated through the difference between CSM and GSM generated from UAV images. A similar study was also carried out by Feng et al. [25], who indicated that the extracted cotton height from UAV images as an important input variable for the cotton production model could help to significantly improve the accuracy of the model. In our study, we also would like to use this approach to extract the sugarcane stalk height from our UAV stereo images for sugarcane yield estimation. Thus, the sugarcane height was computed from the difference of CSM and GSM, as follows, for each pixel:

$$SH = V(CSM) - V(GSM) \tag{1}$$

where SH is the sugarcane height in pixels; V(CSM) and V(GSM) are the pixel values of CSM and GSM images for the corresponding pixels. The raster calculator tool in ARCGIS 10.2 (Esri, Redlands, CA, USA) was used to calculate SH.

2.7. Selection of Vegetation Index for Extraction of Sugarcane Area and Stalk Density Estimation

Extraction of sugarcane planting area is the basis for estimating sugarcane production. Considering the significant difference in reflectance spectra between sugarcane fields and roads, we used the threshold segmentation method to extract the sugarcane planting area in this study and then obtained the distribution of sugarcane plots.

Stalk density in the field is another important variable for sugarcane yield estimation. However, it could be rational to assume that the stalk density of sugarcane farming should be identical to a type of ridge-like planting in the field. However, this assumption might not be true in the field. Many factors control the spatial distribution of sugarcane stalks in the field. One of the direct reasons is that the tiller number of different sugarcane stalks would tend to be different. Therefore, it would be better if we could estimate the stalk

density at the pixel scale for the precision of yield estimation. In this study, we intend to estimate the sugarcane stalk density with vegetation index computable from the obtained UAV orthorectification images, which have 3 bands of red, green, and blue to combine into a true color image. Therefore, we can use the three visible bands to calculate the vegetation indices for the sugarcane stalk density estimation. In order to eliminate the effects of different DN values in each band on the estimation of vegetation indices, normalization of the band DN values is very necessary. For this, we conducted the following normalization before the computation of vegetation indices:

$$R = r/(r + b + g) \tag{2}$$

$$G = g/(r + b + g) \tag{3}$$

$$B = b/(r + b + g) \tag{4}$$

where r, g, and b are the DN values of the original red, green, and blue bands in the UAV images; R, G, and B are the normalized values of the red, green, and blue bands in the UAV image. Several vegetation indices have been developed in the literature for the three visible bands of true color images, for example, the red and green vegetation index (RGVI) proposed by Zhang et al. [26] and the green leaf vegetation index (GLVI) by Louhaichi et al. [27]. In this study, we would like to follow these approaches to calculate the vegetation indices from the three visible bands. Therefore, after normalization was carried out, we computed the following vegetation indices, we also performed filtering operations using threshold segmentation to remove pixels affected by soil background. In this study, we used the following thresholds: if NGVI < 0.20, then NGVI = 0; if NRVI < 0.22, then NRVI = 0; if other indices were less than 0, then they were assigned a value of 0. These operations were implemented using the raster calculator tool in ARCGIS 10.2 (Esri, Redlands, CA, USA).

$$RGVI = (G - R)/(G + R) \tag{5}$$

$$GLVI = (2G - R - B)/(2G + R + B) \tag{6}$$

$$IGRVI = (G^2 - R^2)/(G^2 + R^2) \tag{7}$$

$$NRVI = R/(R + G + B) \tag{8}$$

$$NGVI = G/(R + G + B) \tag{9}$$

$$RGBVI = (G^2 - BR)/(G^2 + BR) \tag{10}$$

where RGVI is the red and green vegetation index [26], GLVI is the green leaf vegetation index [27], IGRVI is the improved green and red vegetation index [28], NRVI and NGVI are the normalized red and green vegetation indices [29], and RGBVI is the visible atmospheric resistance vegetation index [28–30]. Statistical correlation between these vegetation indices and the stalk density was analyzed according to the sampling data from the field. The best one with the highest correlation coefficient would be selected as the independent variable for the stalk density estimation in our study.

2.8. Establishment of Allometric Equation for Variables Estimation

It has been commonly understood that the growth of a plant implies the simultaneous growth of its different parts such as stalk, branches, and leaves, but the growth of these parts is usually at a heterogeneous rate in different growing stages. As to the agricultural crops, the relationship among these parts tends to be the same in the mature stage for harvest. The allometric equation was used to describe this relationship among plant parts for different growing stages [15,16]. Three forms of allometric relationship were commonly used in practice [31–33], of which the following form is the most popular one:

$$Y = a\,X^b \tag{11}$$

where *Y* was the variable representing a biological feature of the plants under study, *a* was a constant of the relationship, *X* was the size of the plant, and *b* was an index relating to allometric growth. Therefore, the coefficients *a* and *b* determined the relationship between the two features *X* and *Y* of the plant. In our study, we would also like to use this allometric relationship to estimate the variables used for sugarcane yield estimation. Python 3.9 was applied to allometric growth equation calculation in this study.

Stalk diameter is also an important variable for cane production estimation. The volume of a sugarcane stalk is governed by its height and diameter. Several studies revealed that the relationship between stalk height and its diameter was not fixed but changed with different growing stages [34–36]. Cheng [36] indicated that the proportion between the height of an individual plant and its total biomass was not at the same rate but as a heterogeneity of 1/4. A study by Hu et al. [37] revealed that the relationship between plant height and diameter of the Machilus pauhoi Kanehira tree tended to be in an elastic form. In our study, we also would like to establish the relationship between the height of the sugarcane stalk and its diameter so that the diameter could be estimated from the remotely extracted stalk height. In addition to this relationship, the allometric equation for stalk diameter and stalk weight would also be examined in our study to see if there was any correlation between the two variables for yield estimation.

Table 2 shows the allometric growth equations using stalk height or stalk height and its diameter to estimate diameter, and the allometric growth formula using stalk height to estimate stalk weight or using stalk height and stalk diameter to estimate stalk weight. There is a good correlation between sugarcane height and diameter (Table 2). Establishing an allometric growth equation for stalk diameter using stalk height, the goodness of fit is higher than 0.77, with the highest goodness of fit reaching 0.89. In stalk weight estimation, we can also see the same effect. Establishing an allometric growth equation for stalk weight using stalk diameter and stalk height, the goodness of fit is higher than 0.7, with the highest goodness of fit reaching 0.91 (Table 2). This suggests that the essential parameters required for accurately estimating sugarcane yield can be efficiently and seamlessly acquired through the application of the allometric growth equation in conjunction with advanced remote sensing technology.

Table 2. Allometric equations to estimate stalk fresh biomass (kg) of sugarcane in study area or all of them combined (general), based on plant height (H, cm) and stalk diameter (D, cm).

Variety	Equation	R^2 *	E_r *	Syx% *
Diameter (cm)	$D = 1.388 \times (DH)^{0.432}$	0.77		
	$D = 1.192 \times (D^2H)^{0.321}$	0.89	3.68	1.73
Stalk weight (kg)	$W = 0.13698 \times (DH)^{1.2965}$	0.91	9.43	1.56
	$W = 0.00166 \times (D^2H)^{0.8985}$	0.90	9.53	1.13
	$W = 1.8835 \times (\ln(D) \times \ln(H))^{0.9811}$	0.88	11.75	2.38
	$W = 2.20719 \times (\ln(H))^{1.883}$	0.73	17.91	5.30
	$W = 0.00009 \times (H)^{1.8219}$	0.73	17.83	4.05

* R^2 = regression coefficient of determination; E_r = relative error of estimate; and Syx% = standard error of variance.

2.9. Development of Sugarcane Yield Estimation Models

According to our above hypotheses about sugarcane production, we can establish the physical model for sugarcane yield estimation as follows:

$$TP = \sum_{1}^{Number} ASW \times SD \tag{12}$$

$$SY = TP/AK \times 10 \tag{13}$$

$$SY_{avg} = \sum_1^j TP_j / \sum_1^j AK_j \qquad (14)$$

where TP is the total production of sugarcane farming in the field, and the number is the total grid number in each plot of the study area. ASW denotes the average weight per stalk (kg) of each grid (1 m $\times$ 1 m), and SD is the sugarcane stalk density in the field of each grid (1 m $\times$ 1 m), i.e., the number of stalks in a unit of cropping acreage.

SY is the sugarcane yield in kilogram per hectare (Mg ha^{-1}), and AK is the acreage of the field (m^2). SY$_{avg}$ denotes the average yield of the study area (Mg ha^{-1}), and j is the total number of sugarcane plots in the study area; here, j = 10. TP$_j$ and AK$_j$ refer to the total production and total area of a certain sugarcane plot in the research area, respectively.

The weight of sugarcane stalk is not easy to estimate. Thus, we can use the variable of crop height for the estimation, as follows:

$$ASW = 0.13698 \times (DH)^{1.2965} \qquad (15)$$

where H represents the average sugarcane stalk height in the field, D is the stalk diameter on average, and ASW is the average stalk weight of sugarcane stalks per square meter. Table 3 shows that there is a close relationship between stalk height and stalk density and, hence, could be estimated with the allometric equations established on the sampling dataset for the entire image on the fields. We choose the highest goodness-of-fit model to estimate sugarcane stalk weight. These operations were completed by Raster calculator and partition statistics using ARCGIS 10.2 (Esri, Redlands, CA, USA).

Table 3. Correlation analysis of the vegetation indices with stalk density in the fields.

No.	Vegetation Indices	Regression Equations	R^2
1	IGRVI	SD = 9.316 $\times$ IGRVI + 1.8108	0.8097
2	RGBVI	SD = 9.068 $\times$ RGBVI + 1.6731	0.7735
3	RGVI	SD = 13.344 $\times$ RGVI + 2.6709	0.7662
4	NRVI	SD = 12.018 $\times$ NRVI + 2.4964	0.7332
5	NGVI	SD = 13.939 $\times$ NGVI $-$ 0.00692	0.7283
6	GLVI	SD = 11.777 $\times$ GLVI + 2.7734	0.6867

Note: SD is stalk density in stalk number per square meter.

2.10. Validation of the Yield Estimation Accuracy

Validation was usually carried out with the following approaches: root mean square error (RMSE), normalized root mean square error (NRMSE), and average absolute estimation error (NAPE). In our study, we also would like to use these approaches for validation of our sugarcane yield estimation and the key variables, as follows:

$$RMSE = \sqrt{\frac{1}{n}\sum_{j=1}^n (X_j - Y_j)^2} \qquad (16)$$

$$NRMSE = RMSE/m \qquad (17)$$

$$NAPE = \frac{1}{n}\sum_{j=1}^n \left(\frac{Y_j - X_j}{Y_j}\right) \qquad (18)$$

where X$_j$ and Y$_j$ represent the estimated and the measured values of the variable for sample j. m is the average measured value of the variable. Since the total planting density samples obtained from field measurement were 57, we divided them into 2 sets: 34 samples for establishment of linear equation for estimation and 23 samples for validation. However, the total stalk weight samples obtained from field measurement and its diameter, height, and canopy height samples were 246; we used 223 samples for the establishment of allometric equations for the estimation and 23 samples for the validation.

3. Results and Analysis

3.1. UAV Mosaic Images of the Region

Figure 1b shows the true color UAV image of the study region. The image covered a region with one big sugarcane field and small parts of other night fields surrounding it (Figure 1b). The two fields in the left lower part of Figure 1b were with an orchard planting Orah mandarin, a typical mandarin orange that became a popular citrus fruit in recent years in Guangxi Zhuang Autonomous Region. In the largest sugarcane field, there is also a small area of Orah mandarin orchard in the lower right corner. Wuming District was famous for its large-scale Orah mandarin farming in Guangxi Zhuang Autonomous Region. The UAV images shown in Figure 1b clearly indicated that the spatial variations in the growth of sugarcane plants across different parts of the fields. The sugarcane in the upper left field next to the citrus field had the worst growing status in comparison to other fields. The big field in the right low part of Figure 1b had a relatively better sugarcane growing status. Field observation found that the sugarcane field next to the citrus orchard was located in a place with a relatively higher altitude in the upper low hill, while the big field in the right lower part of Figure 1b was at a relatively low altitude due to its location in the lower part of the hill, which might have more chance to receive the runoff from the rains. Another feature shown in Figure 1b was the obvious texture of the row form, which properly reflected the ridge-like planting style of sugarcane in the region.

3.2. Sugarcane Stalk Height of the Fields

The sugarcane stalk height of the fields was acquired by the CSM and GSM images of the sugarcane fields. The CSM was generated from the acquired images shown in Figure 1b using the point cloud technique and cloud filtering method from the UAV images, with the 19 ground control points to correct the altitude generated. The GSM was generated from the UAV images acquired after the sugarcane in the field was harvested for the sugar factory when there was no sugarcane left in the fields, so they could be actually viewed as the ground surface with the bare soil surface, and without sugarcane stalk was left in the fields.

Since the CSM reflected the crop canopy altitude extracted from the UAV images while the GSM was the ground surface altitude without the sugarcane plants in the field, the subtraction of the GSM from the CSM would give the sugarcane stalk height in the field. An obvious difference could be seen among the sugarcane canopy heights in the fields. The canopy heights of sugarcane in the north part of the big field were generally greater than in other parts of the field, probably due to the relatively low altitude of the southern parts of the field, which might have better soil fertility and more soil water condition resulting from both runoff and precipitation.

As is known, sugarcane canopy height was not exactly equivalent to the stalk height that could be harvested as the final product of sugarcane farming as raw materials for sugar processing. Usually, there were ~0.5 m from the top of the canopy to the part of the top stalk that could be harvested as the final product for the sugar factory. But, this difference was not identical among the sugarcane plants. Instead, different plants tended to have different distances from the canopy top to the harvested stalk top. Usually, the higher the sugarcane plant, or its canopy height, the higher the harvested stalk. This is especially true for sugarcane, which had better growing status in the field. Due to this fact, the production of sugarcane with taller canopy would tend to have greater harvest production. In order to precisely estimate the sugarcane stalk height from the canopy height extracted from CSM and GSM images, an equation was established with a statistical regression approach using our sampling dataset obtained on the field. Figure 6b shows the plot of measured stalk height against the canopy height extracted from the UAV image in Figure 6a. The linear relationship can be clearly observed between the canopy height and the stalk height. Thus,

the following regression equation was established for the estimation of stalk height from the extracted canopy height image:

$$SH = 0.84004CH + 0.7174 \qquad R^2 = 0.92 \qquad (19)$$

where SH is the sugarcane stalk height, CH is the sugarcane canopy height estimated from the CSM and GSM images, and R^2 is the correlation coefficient of the equation.
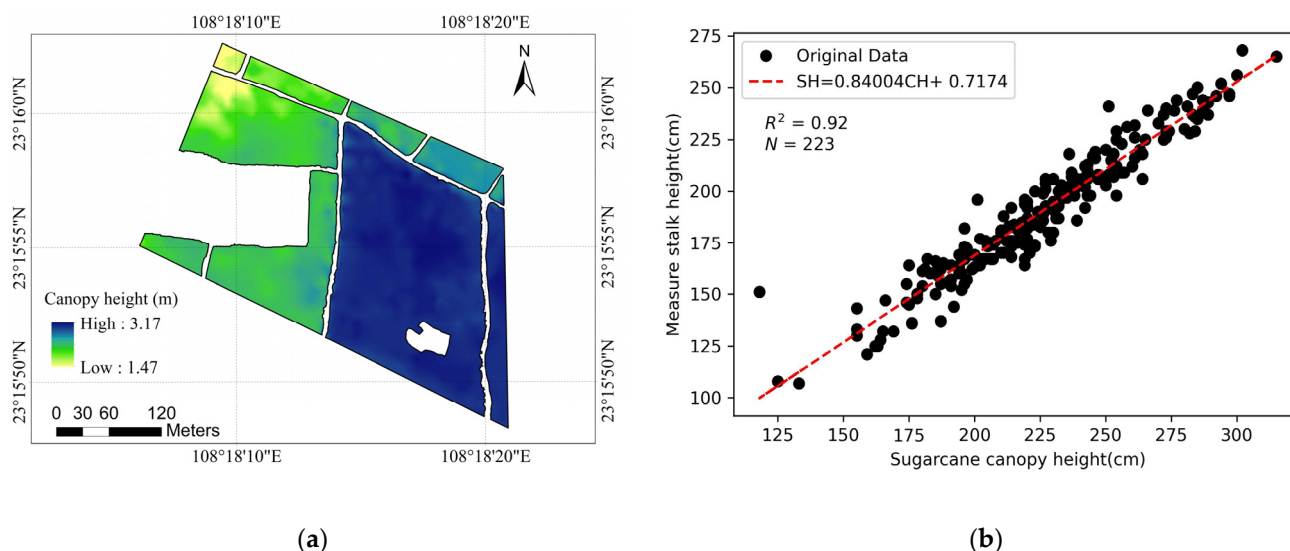

(**a**)   (**b**)

Figure 6. (**a**) Spatial distribution of sugarcane canopy height in the fields. (**b**) The plot of measured stalk height against the canopy height extracted. The regression equation of the canopy height and the stalk height.

3.3. Vegetation Indices for the Study

Figure 7 shows the spatial variation of the six selected vegetation indices in the fields. The indices were computed from the normalization of the original UAV image. All the vegetation indices were able to reflect the sugarcane growing status in the field though obvious differences could be observed for the same vegetation index in the fields. However, one significant feature highlighted in Figure 7 was that the spatial distribution of these vegetation indices in the field tends to be the same, which means that all the vegetation indices were capable of correctly reflecting the growing status of sugarcane in the field. Since the vegetation indices mainly reflect the canopy density in terms of chlorophyll in the field, it might be rationally assumed that the higher the vegetation index, the denser the sugarcane canopy, leading to a closer correlation between the vegetation indices and the crop density in the fields. It was with this assumption that we computed the vegetation indices so that we could select the best vegetation index to establish the model for sugarcane stalk density estimation.

3.4. Models for Stalk Density Estimation

Using the sampling dataset, we correlated the sugarcane stalk density with the extracted vegetation indices. Table 3 shows the results of the correlation. As seen in Table 3, all the vegetation indices had a very close correlation with the stalk density. R^2 of the vegetation indices ranged from 0.6867 to 0.8097. This proved our assumption that vegetation indices were capable of spectrally reflecting the leaf amount of sugarcane canopy, hence, the stalk density in the fields. Detailed examination of Table 3 revealed that IGRVI and RGBVI had the highest R^2, with $R^2 = 0.8097$ and 0.7735, implying the two were the best vegetation indices to establish the models for stalk density in the fields. Therefore, we used the regression equations of the two vegetation indices for stalk density estimation. The

estimated stalk density was computed as the average of the estimation results with the two vegetation indices.
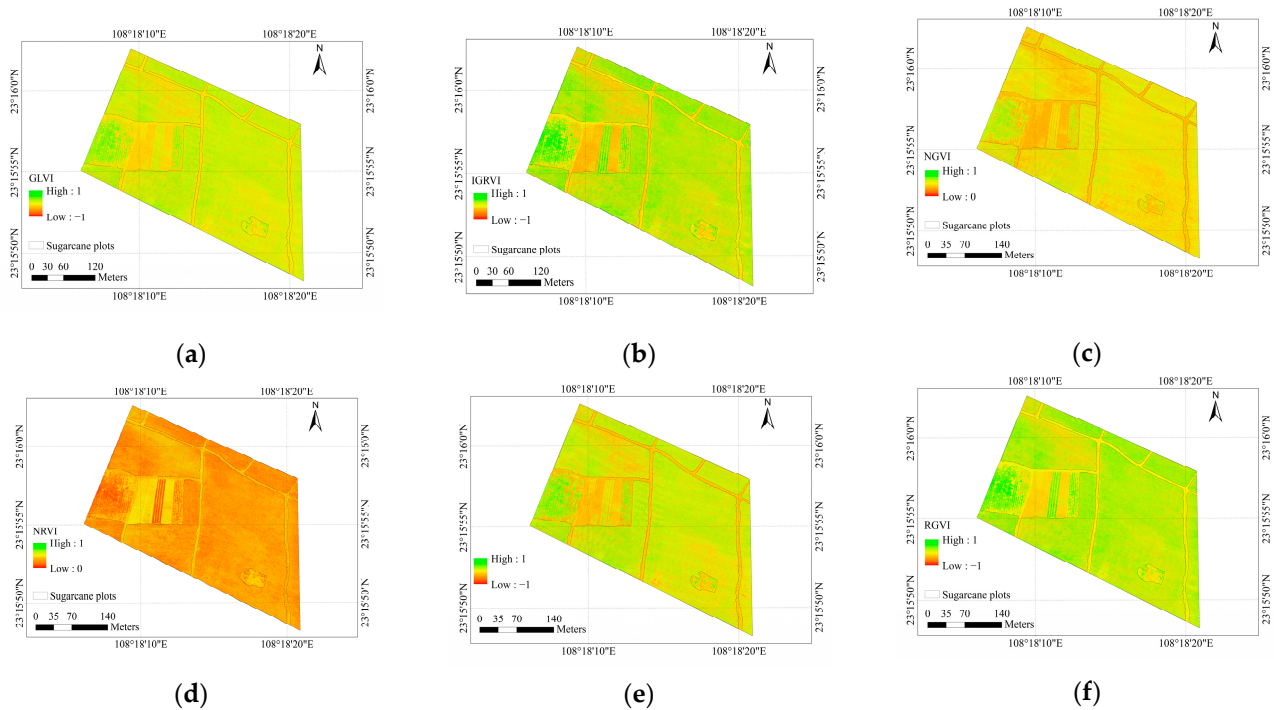

Figure 7. Six selected vegetation indices of fields to reflect the spatial variation of sugarcane canopy density, with (**a**) GLVI, (**b**) IGRVI, (**c**) NGVI, (**d**) NRVI, (**e**) RGBVI, and (**f**) RGVI.

Since sugarcane in the field was planted in the form of ridge-like rows, we used the width between the rows to precisely estimate the stalk density in each row. The regression equations of IGRVI and RGBVI were used to estimate the stalk density in each row. The results are shown in Figure 8a,b. The final results (Figure 8c) were computed as the average of Figure 8a,b. An obvious difference could be observed between the results estimated from the two vegetation indices. Moreover, it could be seen that the stalk density was obviously greater in the upper parts of the fields. Sugarcane plants in these parts were generally above five stalks per square meter, while the left upper part had relatively lower stalk density. The low SD in this part was as low as 2 stalks per square meter. This density difference would have a significant impact on the final production estimated from UAV images.
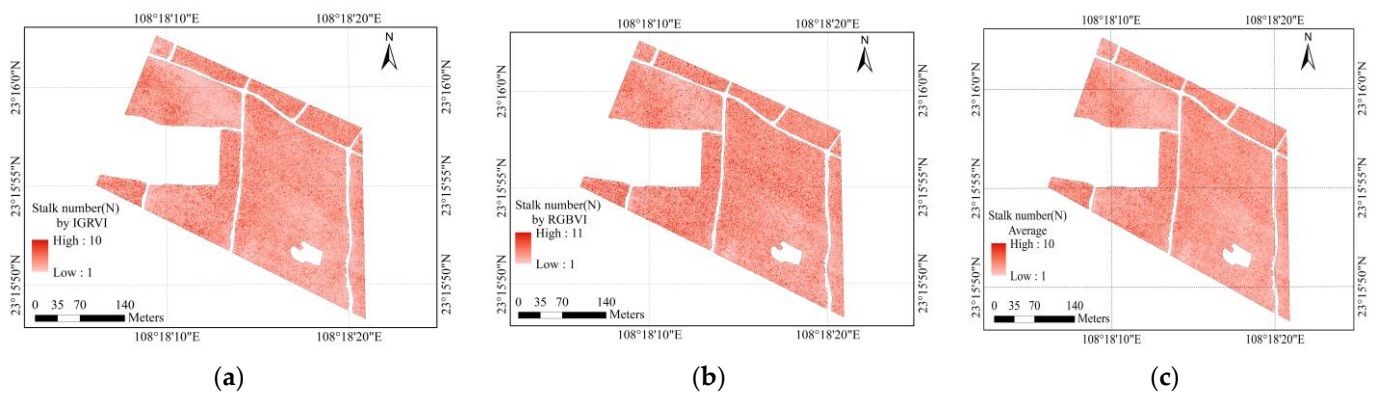

Figure 8. Spatial distribution of sugarcane stalk density in the rows of the sugarcane fields. (**a**) The stalk density estimated with IGRVI, (**b**) from RGBVI, and (**c**) final results of the estimation.

3.5. Allometric Equation for Stalk Height and Diameter

Stalk diameter is also an important factor for precise estimation of sugarcane yield. Using the sampling dataset, we established the allometric equation of stalk height and stalk diameter. Figure 9a shows the relationship between stalk height and diameter of sugarcane. Regression analysis was then used to establish the allometric equation for the two variables, obtaining the result as follows:

$$D = 1.192 \times (D^2H)^{0.321} \qquad R^2 = 0.89 \qquad (20)$$

$$\ln(D) = 0.8966 \times \ln(H) + 0.4906 \qquad (21)$$

where D is stalk diameter in cm and H is stalk height in cm. The R^2 indicates that the stalk height can determine ~90% variance of the sugarcane stalk diameter in the fields, which is high enough for the estimation of sugarcane yield and production. Using this regression equation between stalk height and diameter, we mapped the spatial variation of stalk diameter in the field as shown in Figure 9b. Since the sugarcane was planted in the form of ridge-like rows in the fields, we also followed our procedure to estimate the average diameter of sugarcane stalks in rows as the density did. Figure 9b clearly indicated that the spatial variation of average stalk diameter was far from the same in the field. Instead, remarkable differences can be observed in the distribution of stalk diameters in different parts of the fields. Generally speaking, the diameter ranged from 15 mm to 39 mm with a mean of 27 mm. One feature is that the diameter tended to be smaller in the places where density was high. This probably was due to the fact that the sugarcane stalk in the denser parts would intend to have a rigid environment to compete with the light and nutrition for growing, and, hence, would have a relatively small canopy cover, leading to the relatively small stalk in diameter in comparison to the parts where density was relatively low, and thus had big canopy for obtaining the sunlight and more nutrition for growing.

### 3.6. Estimate Stalk Weight with Stalk Diameter and Stalk Height

The stalk weight of the sugarcane stalk was estimated by the allometric equation (Figure 10b). Figure 10a shows the allometric relationship between sugarcane stalk diameter, stalk height, and stalk weight from the sampling dataset, which was not in a linear form but a non-linear one. Regression of them gave the following equation reflecting their relationship:

$$W = 0.13698 \times (DH)^{1.2965} \qquad R^2 = 0.91 \qquad (22)$$

where W is the stalk weight of sugarcane stalk in kg, D is stalk diameter in cm, and H is stalk height in m. The R^2 of this equation indicated that the stalk diameter can explain ~90% variance of stalk weight among the stalks of sugarcane plants in the fields. Another 10% variance of stalk weight was determined by other variables such as stalk height and stalk density.

3.7. Estimate Sugarcane Yield and Production for the Fields

Sugarcane yield and production of the fields could be estimated with the above allometric variables. Figure 11 shows the spatial variation of the estimated sugarcane yield in the fields. As indicated in Figure 11, the fields in the lower right side of the image had the highest yield, which is high up to 110 Mg ha^{-1}, i.e., 109.34 Mg ha^{-1}. This may be attributed to the location of the field in the lower place in the hills and its relatively better soil fertility. The other fields were estimated with a yield ranging from 60 Mg ha^{-1} to 90 Mg ha^{-1}. In terms of Chinese popular acreage units, the estimated sugarcane yield of the fields was within the range of 60–110 Mg ha^{-1}. This was the normal sugarcane yield in the region. Actually, when conducting the field measurement campaigns, we also chatted with the farming manager of the Farming Base about the growing status of sugarcane farming in the fields. He also gave us a rough estimation of the sugarcane yield as 60–100 Mg ha^{-1} for fields like these in our study region.
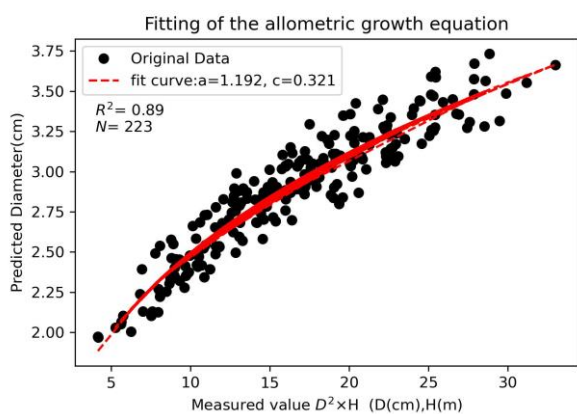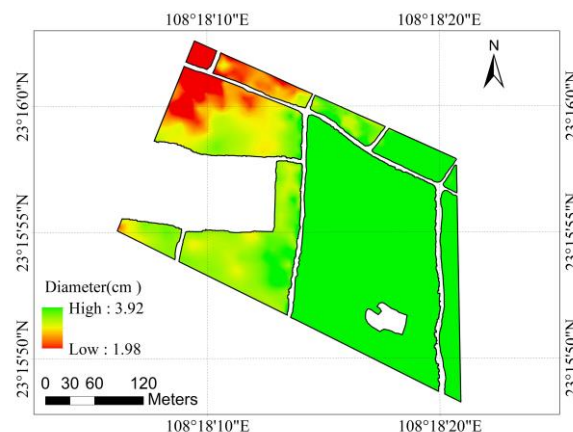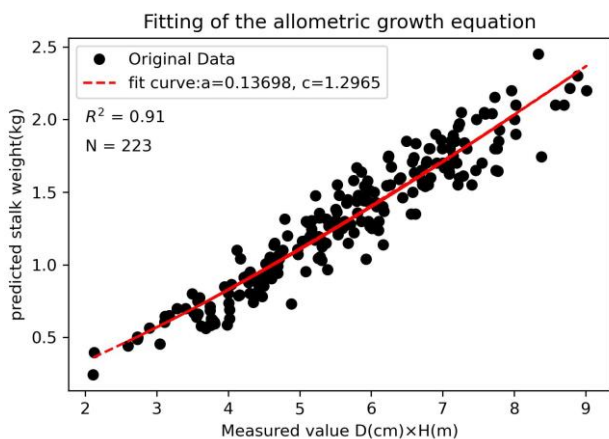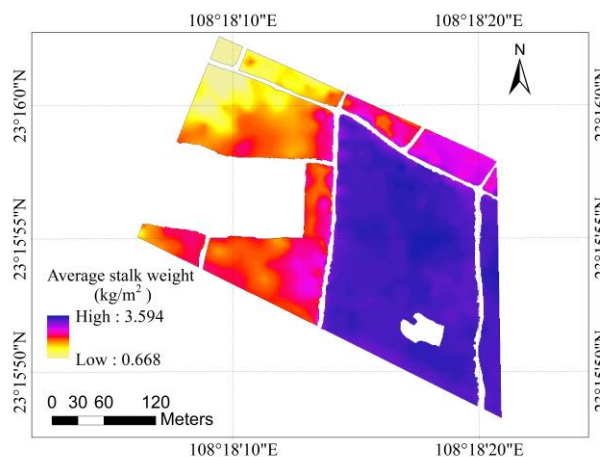
Figure 9. (**a**) Allometric relationship between sugarcane stalk height and diameter from the sampling dataset. (**b**) The estimated stalk diameter in the sugarcane fields.

Figure 10. (**a**) Allometric relationship between sugarcane stalk diameter, stalk height, and stalk weight from the sampling dataset. (**b**) The estimated stalk weight in the fields.

Table 4 lists the results of sugarcane production in the fields within our UAV image coverage, which includes three relatively big fields and parts of the other seven fields. Using the UAV image, we counted the pixels of each field and then calculated their acreage according to the pixel size. Table 4 indicates that the acreage of the 3 big fields was 1.24 ha, 1.35 ha, and 4.023 ha. Other fields only had a part in the image, hence, their acreage was small, i.e., 0.03–0.5 ha. The average yield of these 10 fields was also extracted from the yield image shown in Figure 11. As shown in Table 4, these fields were with average yields in the range of 60–110 Mg ha^{-1}. Since the production of each field was calculated as the acreage multiplied by its average yield, we obtained the total production in the study area as 775.96 Mg. The production for the three big fields was 87.96 Mg, 107.64 Mg, and 439.88 Mg. This precise estimation of sugarcane yield and production can provide very useful information for the farmers to estimate their expectation of the farming income and for the sugar processing mill to make decisions on the harvesting schedule for the sugarcane farmers in its raw material hinterland.
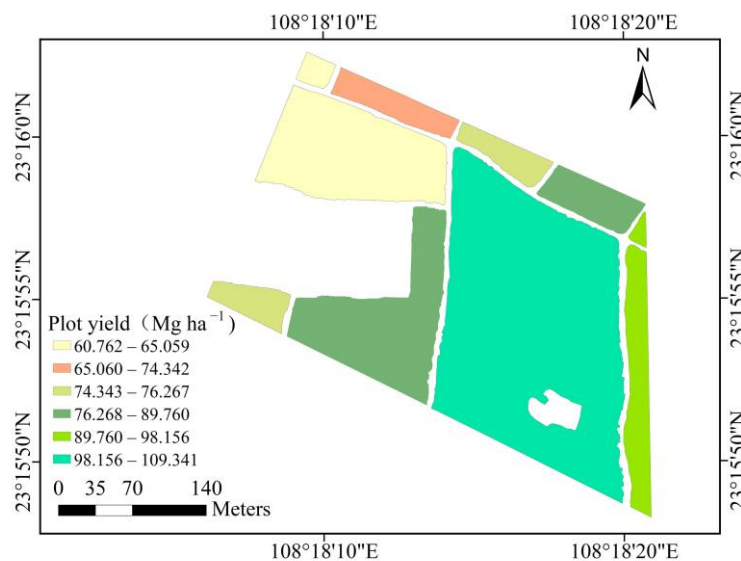
Figure 11. The estimated sugarcane yield in the fields.

Table 4. The estimated sugarcane yield and production of the fields.

Field No.	Acreage (m²)	Acreage (ha)	Yield (kg m⁻²)	Yield (Mg ha⁻¹)	Production (Mg)	Measured Yield (Mg ha⁻¹)
1	2102	0.210	7.63	76.27	16.02	75.18
2	13,522	1.352	6.51	65.06	87.96	62.88
3	2827	0.283	7.43	74.34	21.04	70.68
4	2137	0.214	7.54	75.36	16.13	72.46
5	40,232	4.023	10.93	109.34	439.88	104.84
6	3257	0.326	8.98	89.76	29.26	85.28
7	12,406	1.241	8.67	86.73	107.64	79.40
8	323	0.032	9.76	97.55	3.12	85.30
9	5099	0.510	9.82	98.16	50.06	90.17
10	795	0.080	6.08	60.76	4.86	58.03
Total (Mg)	82,700	8.270			775.96	
Average yield (Mg ha⁻¹)					93.83	89.21

3.8. Validation of the Yield and Production Estimation

Validation of this study was carried out in two ways: through the allometric variables and the final yield and production. As outlined above, the sugarcane yield and production were estimated through an approach of allometric variables that determine the yield and production in the fields. Thus, we can split the sampling dataset into two parts: one for model establishment and the other for validation. Using the validation dataset from field sampling campaigns, we can validate the estimation accuracy of the required variables for the yield and production. Figure 12 shows the validation of stalk height, diameter, density, and stalk weight. As seen in Figure 12, the RSME of sugarcane stalk height, diameter, density, and stalk weight in the fields was 0.28, 0.33, 1.34, and 0.22, respectively. The relatively small RMSE indicates that the estimation of these four allometric variables was high enough for a precise estimation of sugarcane yield and production in the study region. The other two validation parameters NRMSE and NAPE also showed the high estimation accuracy of the four variables.

For the validation by yield and production, we followed the general approach of ground estimation of sugarcane yield and production through field measurements to use our sampling measurements on stalk height, diameter, density, and stalk weight of the fields to compute their average and then apply these average measurements to calculate the yield and production of the fields. The estimation accuracy is RMSE = 6.63 Mg ha⁻¹, implying

that our estimation of sugarcane yield in the study would have an average error of ~6.6 Mg ha^{-1}. Provided the average yield of sugarcane was usually high up to 60–110 Mg ha^{-1}, this estimation with the proposed methodology in this study was precise enough for practical applications. The other two validation coefficients NRMSE and NAPE also indicated the high accuracy of the estimation. The normalized root mean square error is NRMSE = 0.0743, implying that the yield estimation accuracy is high, up to $(1 - 0.0743) \times 100 = 92.57\%$. The average absolute estimation error NAPE = -0.0608 indicated that the yield estimation was with an over value to the actual yield by 6.08%, which is quite small in comparison to sugarcane yield. Therefore, we can conclude that our estimation of sugarcane yield and production using this approach is precise enough for practical applications.
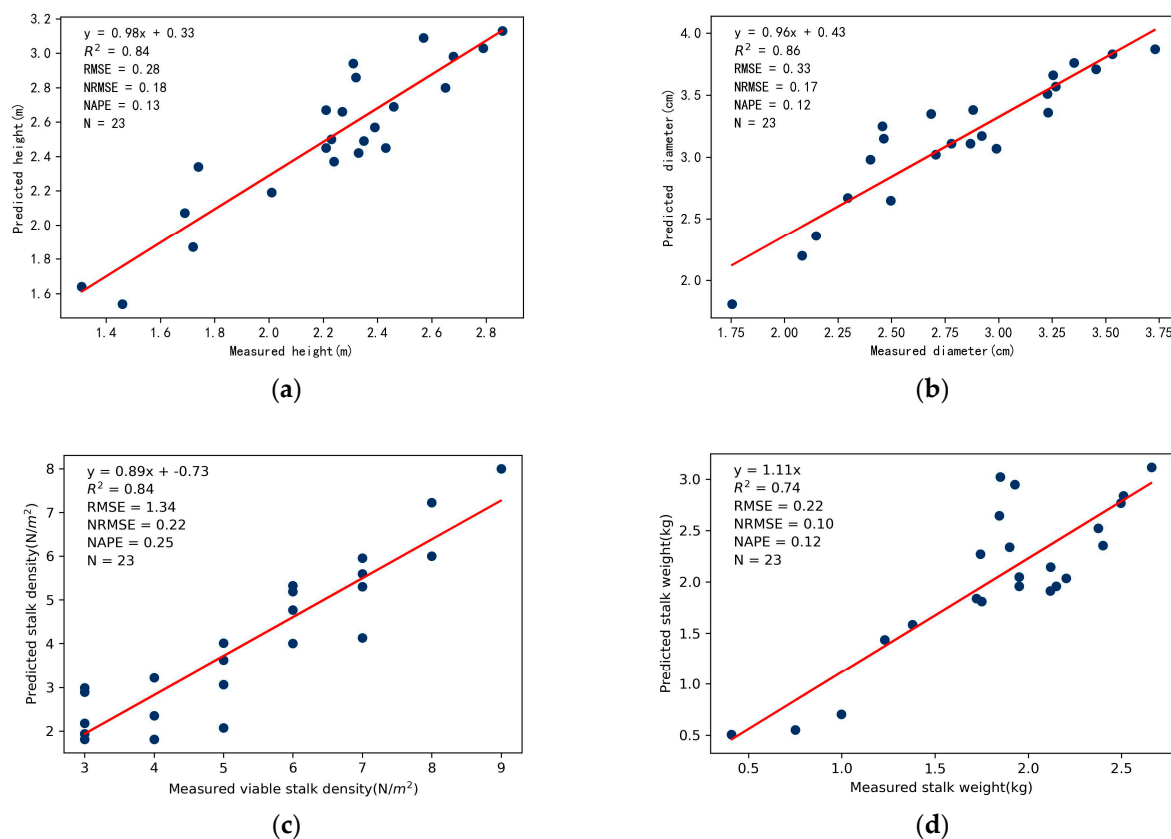

Figure 12. Validation of the allometric variables by plotting their estimation and measurement from the field sampling campaigns for stalk height (**a**), diameter (**b**), density (**c**), and stalk weight (**d**).

4. Discussion

Due to its convenience, easy operation, and high spatial resolution, UAV remote sensing applications have gained rapid development in recent years. Precise estimation of crop yield and production represents one such application with UAV remote sensing. In our study, we conducted the experimental study of applying the very-high-spatial-resolution UAV RGB image to estimate sugarcane yield and production at field scales through the approach to extract allometric variables of sugarcane farming for a precise estimation of the sugarcane yield and production in the experimental fields. Even though the validation indicated that the approach was feasible and applicable for practical purposes, uncertainty could still be seen in the various procedures of study that might affect the final result of the sugarcane yield and production estimation. We understand that several factors might serve as critical to the uncertainty of the yield and production estimation.

Since the study was based on UAV images, the accuracy of UAV image acquisition would play a key role in the functions leading to the uncertainty of the estimation. Generally speaking, the UAV technology has been developed into a new generation tool to obtain

very-high-spatial-resolution images for various applications. However, due to its light and low flight altitude, the selection of good weather and a skillful operator is very important to obtain the required UAV images for sugarcane yield estimation. This might include several aspects: (a) a decision on which days are rightly proper for the observation of the image; (b) UAV flight height and frequency of photo taking so that the mosaic image could be generated with high quality; (c) UAV camera for the photo taking; (d) ground control points; and (e) the programs used for the mosaic of the photos into the orthorectification images. These aspects are very important in producing high-quality UAV images for the application. In our study, we only had a general UAV color camera to take the RGB photos. Thus, we did not have a near-infrared band for a better approach to compute the required vegetation indices for crop variable estimation.

Field sampling is also very important in this study. As seen above, the field sampling data were used to develop models for allometric variable extraction, as well as to validate the results of the variable extraction and yield estimation. Actually, sugarcane field measurements were very hard to conduct due to the density of sugarcane plants in the field and the height of sugarcane stalks. For each sampling point, we had to take five plants to measure their stalk height, canopy height, and stalk diameters at three levels. Therefore, the selection of the five plants was very important because they were selected to represent the sugarcane plants at the sampling site. Moreover, we also needed to count the number of sugarcane plants in two adjacent rows, measure the width between the two adjacent rows for the density, and cut one or two plants to weigh how heavy it is so that the specific gravity could be calculated. In addition, geographic coordinate was also required to be recorded. Therefore, it is very hard to have enough sampling points for practical applications. In our study, we have four persons to work three days in the three fields for the sampling. Only 57 sampling points were completed by the campaign. This sampling number was not very large and might not be a very good representative of the sugarcane farming in the fields. Moreover, we also understand that the field sampling measurement would surely involve a certain level of errors affecting our estimation accuracy of the sugarcane yield and production in the fields. This was why our yield estimation was with an accuracy of ~93% or an error of 7% as indicated by the validation.

The final factor affecting the final estimation of sugarcane yield and production in this study was the approach to generate the CSM and GSM images for stalk height estimation and to establish the allometric equations for crucial variable estimation. In this study, we followed the general approach of point cloud segmentation and point filtering methods for CSM and GSM generation. Previous studies [15,32] also indicated that the accuracy of CSM generation directly affected the estimation of biomass in their studies. Moreover, it is necessary to highlight that the way to establish the allometric equations for the estimation of crucial variables is also very important to affect the yield estimation with an allometric approach. In our study, we used the stalk height as the key determinant for other allometric variables. This application involved an implicit assumption that the height was directly related to the variance of another allometric variable, such as diameter. This might not be very true in the field because the density, crop variety, soil fertility, rainfall, and many other climate factors also played important roles in shaping the change of stalk diameter in the fields. This complicated relationship among the allometric variables made the efforts to establish the required regression equation using one or two variables to estimate the other difficult in the real world. However, our study also revealed that such an effort was worthy of examination since it provided an alternative for simplifying the complicated relationship so that the allometric approach could be used for practical use.

Another factor impacting the remote sensing estimation of sugarcane yield was the lodging of sugarcane stalks caused by strong winds or typhoons, which was generally observed in the subtropical sugarcane growing region in Guangxi, South China, where strong winds or typhoons were a commonly occurring disaster weather in the summer season, especially during July and August. This study was conducted on the general sugarcane growing fields without obvious stalk lodging, hence, without accounting for

the possible impact of lodging on yield estimation results of our UAV remote sensing. However, it is important to note that lodging has a significant impact on the estimation of sugarcane yield using remote sensing techniques [1,8]. Lodging modifies various aspects of the original reflectance spectrum, vegetation index, texture characteristics, canopy coverage, digital surface model, and other factors that are utilized for the estimation of sugarcane stalk density, height, and other parameters [7,8]. Generally, there was about a 20% loss of sugarcane yield when a moderate level of lodging happened Guangxi sugarcane growing region in South China. Therefore, it still remains a much more complicated and challenging task to precisely estimate sugarcane yield with remote sensing techniques under lodging conditions.

5. Conclusions

Sugarcane yield estimation was examined in the study through an allometric approach revealing the mutual relationships among the crucial variables of the crop. Using the sampling dataset, allometric equations reflecting the mutual relationship among stalk height, stalk diameter, and stalk weight were established for the estimation of the required variables. Our results indicated that the spatial distribution of stalk height, stalk diameter, and stalk weight was an obvious feature of heterogeneity in different parts of the fields. The correlation between stalk height and diameter is positive but it is negative between the diameter and the density. This finding exactly reveals the principle behind the generally observed phenomenon of the relationship between the two variables, which is that crop plants tend to grow stronger in the part of the fields with sparser crop plants.

The acreage of the fields could be statistically calculated according to the pixel numbers and pixel size of the fields in the UAV image. Statistics indicated that the 3 big fields were with an acreage of 1.24 ha, 1.35 ha, and 4.023 ha, respectively. The total production in the study area was accordingly estimated as 775.96 Mg. The production for the three big fields was 87.96 Mg, 107.64 Mg, and 439.88 Mg. This precise estimation of sugarcane yield and production is very useful to both the farmers and the sugar processing mill.

Validation with the sampling dataset indicated that the RSME of sugarcane stalk height, diameter, density, and stalk weight in the fields was small, i.e., RMSE = 6.63 Mg ha^{-1}. Provided that sugarcane farming in the region would usually have a yield of 60–110 Mg ha^{-1}, this estimation with our approach was precise enough for practical applications. Validation with NRMSE resulted in NRMSE = 0.0743, implying that the yield estimation accuracy is high up to 92.57%. Another validation coefficient was NAPE = −0.0608, implying that our estimation was with an underestimation of the actual yield by ~6.08%, which is quite small in comparison to sugarcane yield. Therefore, it could be concluded that the approach presented in the study might serve as a potential alternative with UAV images for precise estimation of sugarcane yield and production in field scale for practical applications.

the allowance for and assistance with UAV photo taking and field sampling campaigns in the fields on their Dongfeng Sugarcane Farming Base.

Conflicts of Interest: The authors declare no conflicts of interest.

References

1. He, Y.; Pan, X.; Pei, Z.; Ma, S.; MaNirn, H.; Shang, J. Estimation of LAI and Yield of Sugarcane Based on SPOT Remote Sensing Data. *Trans. Chin. Soc. Agric. Mach.* **2013**, *44*, 226–231.
2. Xu, J.; Ma, J.; Tang, Y.; Wu, W.; Shao, J.; Wu, W.; Wei, S.; Liu, Y.; Wang, Y.; Guo, H. Estimation of sugarcane yield using a machine learning approach based on UAV-LiDAR Data. *Remote Sens.* **2020**, *12*, 2823. [CrossRef]
3. Som-ard, J.; Hossain, M.D.; Ninsawat, S.; Veerachitt, V. Pre-harvest sugarcane yield estimation using UAV-based RGB images and ground observation. *Sugar Tech.* **2018**, *20*, 645–657. [CrossRef]
4. Sanches, G.M.; Duft, D.G.; Kölln, O.T.; Luciano, A.C.D.S.; De Castro, S.G.Q.; Okuno, F.M.; Franco, H.C.J. The potential for RGB images obtained using unmanned aerial vehicle to assess and predict yield in sugarcane fields. *Int. J. Remote Sens.* **2018**, *39*, 5402–5414. [CrossRef]
5. Sumesh, K.C.; Ninsawat, S.; Som-ard, J. Integration of RGB-based vegetation index, crop surface model and object-based image analysis approach for sugarcane yield estimation using unmanned aerial vehicle. *Comput. Electron. Agric.* **2021**, *180*, 105903.
6. Yu, D.; Zha, Y.; Shi, L.; Jin, X.; Hu, S.; Yang, Q.; Huang, K.; Zeng, W. Improvement of sugarcane yield estimation by assimilating UAV-derived plant height observations. *Eur. J. Agron.* **2020**, *121*, 126159. [CrossRef]
7. Chea, C.; Saengprachatanarug, K.; Posom, J.; Wongphati, M.; Taira, E. Sugar yield parameters and fiber prediction in sugarcane fields using a multispectral camera mounted on a small unmanned aerial systalk (UAS). *Sugar Tech.* **2020**, *22*, 605–621. [CrossRef]
8. Shendryk, Y.; Sofonia, J.; Garrard, R.; Rist, Y.; Skocaj, D.; Thorburn, P. Fine-scale prediction of biomass and leaf nitrogen content in sugarcane using UAV LiDAR and multispectral imaging. *Int. J. Appl. Earth. Obs. Geoinf.* **2020**, *92*, 102177. [CrossRef]
9. de Oliveira, R.P.; Barbosa Júnior, M.R.; Pinto, A.A.; Oliveira, J.L.P.; Zerbato, C.; Furlani, C.E.A. Predicting sugarcane biometric parameters by UAV multispectral images and machine learning. *Agronomy* **2022**, *12*, 1992. [CrossRef]
10. Akbarian, S.; Jamnani, M.R.; Xu, C.; Wang, W.; Lim, S. Plot level sugarcane yield estimation by machine learning on multispectral images: A case study of Bundaberg, Australia. *Inf. Process. Agric.* **2023**. [CrossRef]
11. Barbosa Júnior, M.R.; Moreira, B.R.D.A.; de Oliveira, R.P.; Shiratsuchi, L.S.; da Silva, R.P. UAV imagery data and machine learning: A driving merger for predictive analysis of qualitative yield in sugarcane. *Front. Plant Sci.* **2023**, *14*, 1114852. [CrossRef] [PubMed]
12. Hiernaux, P.; Issoufou, H.B.A.; Igel, C.; Kariryaa, A.; Kourouma, M.; Chave, J.; Mougin, E.; Savadogo, P. Allometric equations to estimate the dry mass of Sahel woody plants mapped with very-high resolution satellite imagery. *For. Ecol. Manag.* **2023**, *529*, 120653. [CrossRef]
13. de Carvalho, E.X.; Menezes, R.S.C.; de Sá Barreto Sampaio, E.V.; Neto, D.E.S.; Tabosa, J.N.; de Oliveira, L.R.; Simões, A.L.; Sales, A.T. Allometric Equations to Estimate Sugarcane Aboveground Biomass. *Sugar Tech.* **2019**, *21*, 1039–1044. [CrossRef]
14. Antunes, W.C.; Pompelli, M.F.; Carretero, D.M.; DaMatta, F.M. Allometric models for non-destructive leaf area estimation in coffee (Coffea arabica and Coffea canephora). *Ann. Appl. Biol.* **2008**, *153*, 33–40. [CrossRef]
15. Vargas-Larreta, B.; López-Sánchez, C.A.; Corral-Rivas, J.J.; López-Martínez, J.O.; Aguirre-Calderón, C.G.; Álvarez-González, J.G. Allometric equations for estimating biomass and carbon stocks in the temperate forests of North-Western Mexico. *Forests* **2017**, *8*, 269. [CrossRef]
16. Youkhana, A.H.; Ogoshi, R.M.; Kiniry, J.R.; Meki, M.N.; Nakahata, M.H.; Crow, S.E. Allometric models for predicting aboveground biomass and carbon stock of tropical perennial C4 grasses in Hawaii. *Front. Plant Sci.* **2017**, *8*, 650. [CrossRef] [PubMed]
17. Tucker, C.; Brandt, M.; Hiernaux, P.; Kariryaa, A.; Rasmussen, K.; Small, J.; Igel, C.; Reiner, F.; Melocik, K.; Meyer, J.; et al. Sub-continental-scale carbon stocks of individual trees in African drylands. *Nature* **2023**, *615*, 80–86. [CrossRef]
18. National Bureau of Statistics of China. *China Statistics Yearbook-2022*; China Statistics Press: Beijing, China, 2023. Available online: http://www.stats.gov.cn/sj/ndsj/2022/indexch.htm (accessed on 3 December 2023).
19. Historical Records Office of Wuming District of Nanning City. Basic Overview of Wuming District of Nanning City. Available online: http://www.wuming.gov.cn/wmgk/wmgk/t397795.html (accessed on 1 December 2023).
20. Guo, T.; Yan, A.; Geng, H. Prediction of Wheat Plant Height and Leaf Area Index Based on UAV Image. *J. Triticeae Crops* **2020**, *40*, 1129–1140.
21. Zarco-Tejada, P.J.; Diaz-Varela, R.; Angileri, V.; Loudjani, P. Tree Height Quantification Using Very High Resolution Imagery Acquired from an Unmanned Aerial Vehicle (UAV) and Automatic 3D Photo-Reconstruction Methods. *Europ. J. Agron.* **2014**, *55*, 89–99. [CrossRef]
22. Zhang, L.; Grift, T.E. A LIDAR-Based Crop Height Measurement System for Miscanthus Giganteus. *Comput. Electron. Agri.* **2012**, *85*, 70–76. [CrossRef]
23. Selkowitz, D.J.; Green, G.; Peterson, B.; Wylie, B. A Multi-Sensor Lidar, Multi-Spectral and Multi-Angular Approach for Mapping Canopy Height in Boreal Forest Regions. *Remote Sens. Environ.* **2012**, *121*, 458–471. [CrossRef]
24. Zhang, H.; Tan, Z.; Han, W.; Zhu, S.; Zhang, S.; Ge, C. Extraction method of maize height based on UAV remote sensing. *Trans. Chin. Soc. Agric. Mach.* **2019**, *50*, 241–250.

25. Feng, A.; Zhang, M.; Sudduth, K.A.; Vories, E.D.; Zhou, J. Cotton yield estimation from UAV-based plant height. *Trans. ASABE* **2019**, *62*, 393–404. [CrossRef]

26. Zhang, J.; Qiu, X.; Wu, Y.; Zhu, Y.; Cao, Q.; Liu, X.; Cao, W. Combining texture, color, and vegetation indices from fixed-wing UAS imagery to estimate wheat growth parameters using multivariate regression methods. *Comput. Electron. Agric.* **2021**, *185*, 106138. [CrossRef]

27. Louhaichi, M.; Borman, M.M.; Johnson, D.E. Spatially located platform and aerial photography for documentation of grazing impacts on wheat. *Geocarto. Int.* **2001**, *16*, 65–70. [CrossRef]

28. Bendig, J.; Yu, K.; Aasen, H.; Bolten, A.; Bennertz, S.; Broscheit, J.; Gnyp, M.L.; Bareth, G. Combining UAV-based plant height from crop surface models, visible, and near infrared vegetation indices for biomass monitoring in barley. *Int. J. Appl. Earth Obs. Geoinf.* **2015**, *39*, 79–87. [CrossRef]

29. Kawashima, S.; Nakatani, M. An algorithm for estimating chlorophyll content in leaves using a video camera. *Ann. Bot.* **1998**, *81*, 49–54. [CrossRef]

30. Gitelson, A.A.; Kaufman, Y.J.; Stark, R.; Rundquist, D. Novel algorithms for remote estimation of vegetation fraction. *Remote Sens. Environ.* **2002**, *80*, 76–87. [CrossRef]

31. Choi, H.I. Parameterization of high resolution vegetation characteristics using remote sensing products for the Nakdong River Watershed, Korea. *Remote Sens.* **2013**, *5*, 473–490. [CrossRef]

32. Kajimoto, T.; Matsuura, Y.; Osawa, A.; Abaimov, A.P.; Zyryanova, O.A.; Isaev, A.P.; Yefremov, D.P.; Mori, S.; Koike, T. Size–mass allometry and biomass allocation of two larch species growing on the continuous permafrost region in Siberia. *Forest. Ecol. Manag.* **2006**, *222*, 314–325. [CrossRef]

33. Li, C.; Li, G.; Xiao, C. The application of allometric relationships in biomass estimation in terrestrial ecosystalks. *World Sci-Tech RD* **2007**, *29*, 51–57.

34. Zuo, S.; Ren, Y.; Weng, X.; Ding, H.; Luo, Y. Biomass allometric equations of nine common tree species in an evergreen broadleaved forest of subtropical China. *Chin. J. Appl. Ecol.* **2015**, *26*, 356–362.

35. Lin, K.; Lyu, M.; Jiang, M.; Chen, Y.; Li, Y.; Chen, G.; Xie, J.; Yang, Y. Improved allometric equations for estimating biomass of the three Castanopsis carlesii H. forest types in subtropical China. *New For.* **2017**, *48*, 115–135. [CrossRef]

36. Cheng, D. Plant Allometric Study of Biomass Allocation Pattern and Biomass Production Rates. Ph.D. Thesis, Lanzhou University, Lanzhou, China, 2007; p. 97.

37. Hu, B.; Zhong, Q.; Cheng, D.; Su, Y.; Xu, C. Relationship between Machilus' height and allometric growth of diameter at breast. *J. Shenyang Univ. (Nat. Sci.)* **2012**, *24*, 9–14.